Biomimetic Catalysis

DOI: 10.1002/anie.201108400

Graphene-Supported Hemin as a Highly Active Biomimetic Oxidation Catalyst**

Teng Xue, Shan Jiang, Yongquan Qu, Qiao Su, Rui Cheng, Sergey Dubin, Chin-Yi Chiu, Richard Kaner, Yu Huang, and Xiangfeng Duan**

Using synthetic systems to mimic natural enzymes with high catalytic activity and distinct substrate selectivity has been a challenge for the last decades. Hemin, the catalytic center for many protein families including cytochromes, peroxidases, myoglobins, and hemoglobins, can catalyze a variety of oxidation reactions like peroxidase enzymes.[1] However, direct application of hemin as an oxidation catalyst is of significant challenge because of its molecular aggregation in aqueous solution to form catalytic inactive dimers and oxidative self-destruction in the oxidizing media, which causes passivation of its catalytic activity.[2] A potential solution to this problem is to synthetically modify the porphyrin structure to achieve a variety of iron porphyrin derivatives for improved catalytic activity or stability.[3] An alternative approach is to use high surface area materials such as zeolites, nanoparticles, silica, or natural clay to support hemin to achieve improved stability or activity in epoxidation or other reactions in organic solutions.[4] For reactions in aqueous solutions, hydrogel-embedded hemin[5] or more elaborate hemin complexes obtained by conjugating with specific antibodies[6] have shown activities significantly better than free molecules, which is, however, still orders of magnitude inferior to natural enzymes, not to mention the difficulties in the synthesis of such kinds of complex hemin conjugates. Therefore, the discovery and development of novel materials as supports to achieve biomimetic catalysts with enzyme-like activity is highly desired.

Graphene, a single layer of carbon arranged in a honeycomb structure, has attracted intense interest because of its fascinating electronic, thermal, and mechanical properties.[7] Graphene is typically prepared through mechanical cleavage or chemical methods.[8] In particular, chemical exfoliation of graphite oxide (GO) either by ultrasonic dispersion or rapid thermal expansion followed by chemical reduction provides a low-cost and scalable method to produce bulk quantities of graphene flakes for a wide range of applications.[9] The resulting graphene usually has a rich variety of surface defects and functional groups such as carboxylic groups to enable its dispersion in aqueous solution.[9a,b] With a two-dimensional sheet-like structure, graphene represents an interesting geometrical support for molecular catalysts with a large open surface area that is readily accessible to substrates/products with a small diffusion barrier, which is distinct from conventional high surface area porous materials. Moreover, graphene also possesses a rich surface chemistry and has the potential to further promote the catalytic activity and stability of the supported molecular systems such as hemin and other porphyrin species through cation–π interactions or π–π stacking. Although the formation of porphyrin–graphene heterostructures[10] and their electrochemical applications[11] have been reported recently, many of these studies involve catalytically less active dimers[10d,11c] and the superior catalytic properties of hemin–graphene conjugates have not yet been adequately explored.

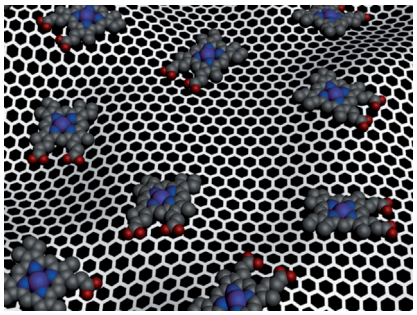

Figure 1. Formation of hemin–graphene conjugates through π–π stacking interactions.

Here we report the synthesis of a hemin–graphene conjugate (Figure 1) through π–π stacking interactions. Spectroscopic characterizations show that hemin retains the catalytic-active monomer form as in natural enzymes. The catalytic studies show that the hemin–graphene conjugates can function as effective catalysts in the oxidation reaction of pyrogallol with exceptionally high catalytic activity (k_{cat}) and substrate binding affinity (K_M) approaching that of natural enzymes. An iron–porphyrin derivative, tetramethylpyridylporphyrin iron (FeTMPyP), was also immobilized on graphene with nearly enzyme-like activity, demonstrating the general applicability of graphene as a support for metalloporphyrin species.

[*] T. Xue, R. Cheng, C.-Y. Chiu, Prof. Y. Huang
Department of Materials Science and Engineering
University of California, Los Angeles, CA 90095 (USA)
E-mail: yhuang@seas.ucla.edu

S. Jiang, Dr. Y. Qu, Q. Su, S. Dubin, Prof. R. Kaner, Prof. X. Duan
Department of Chemistry and Biochemistry
University of California, Los Angeles, CA 90095 (USA)
E-mail: xduan@chem.ucla.edu

Prof. R. Kaner, Prof. Y. Huang, Prof. X. Duan
California Nanosystems Institute, University of California
Los Angeles, CA 90095 (USA)

[**] We acknowledge financial support of this work by the National Science Foundation (CBET1033672, DMR0956171) and the National Institutes of Health (1DP2OD004342-01).

Supporting information for this article is available on the WWW under http://dx.doi.org/10.1002/anie.201108400.

WILEY ONLINE LIBRARY

© 2012 Wiley-VCH Verlag GmbH & Co. KGaA, Weinheim

Graphene oxide is prepared through Hummer's method[12] and graphene is obtained by reducing graphene oxide with hydrazine.[9b] The graphene solution was directly used for the subsequent studies without further purification. Because of the insolubility of hemin in neutral aqueous solution, the conjugation experiments between hemin and graphene were carried out in methanol. The hemin–graphene conjugates were prepared by dispersing dry graphene in 1.5 mM hemin in methanol followed by incubation for 120 min. The hemin–graphene conjugates were then separated from the reaction solution through a centrifugation process, and characterized using UV/Vis spectroscopy and atomic force microscopy (AFM).

UV/Vis absorption spectra of the hemin methanol solution, a mixture of hemin and graphene in methanol, and separated hemin–graphene conjugates re-dispersed in methanol show nearly the same absorption characteristics with a Soret band at 400 nm (Figure 2a). The absorption band is consistent with that of monomeric hemin in methanol or dimethyl sulfoxide solution,[13] suggesting that the adsorbed hemin species on graphene are monomeric—the same form that hemin takes in natural enzymes. This is also distinct from previous studies on graphene–hemin conjugates, in which hemin dimers are typically obtained.[10d,11c] A careful analysis of the spectra reveals that there is a spectral shift in the Q bands and charge-transfer band upon the formation of the graphene–hemin conjugate. For example, the Q bands of hemin in the hemin–graphene conjugate are blue-shifted from 504 to 501 nm and from 535 to 531 nm, respectively, compared to free hemin. The charge-transfer band shows an even clearer blue-shift from 628 to 623 nm (Figure 2b). The band shift suggests the formation of an axial ligation to the iron center of hemin[14] likely because of cation–π interactions between iron centers and graphene.

The separated hemin–graphene conjugates were then re-dispersed in pH 7.4 Tris buffer. The equivalent amount of free hemin was also dispersed in pH 7.4 Tris buffer to form a saturated solution. The UV/Vis absorption spectra of hemin–graphene conjugates in pH 7.4 Tris buffer show the same absorption peaks as that in methanol, confirming the structural stability of the hemin–graphene conjugates in pH 7.4 Tris buffer. Quantitative analysis shows that the coverage of hemin on graphene in hemin–graphene conjugates is around 0.3 monolayer (see the Experimental Section in the Supporting Information). In contrast, the free hemin solution in pH 7.4 Tris buffer shows an extremely weak absorption at 385 nm, indicating the low solubility of hemin and formation of catalytically inactive dimers.[15]

The absorption of a hemin monolayer on graphene was also investigated by AFM studies. Specifically, graphene was first deposited onto a silicon oxide substrate from aqueous solution. AFM images were then used to determine the thickness of the selected graphene flakes (around 1.6 nm for three to four layers of graphene as shown in Figure 3a and around 1.4 nm for two to three layers of graphene as shown in Figure 3b). The substrate was then immersed into the hemin–methanol solution to allow for absorption of hemin on graphene. The absorption of hemin on a bare silicon oxide substrate is nearly negligible in this process (see Figure S1 in the Supporting Information). After absorption, AFM studies show that the thickness of exactly the same graphene flakes (around 2.0 nm in Figure 3a and around 1.8 nm in Figure 3b, respectively) is increased by around 0.4 nm, which can be attributed to the absorption of a monolayer of hemin molecules on graphene. Control studies conducted by immersing graphene into pure methanol show no change in the thickness (Figure S2 in the Supporting Information), confirming the thickness increase observed above is indeed because of the absorption of hemin on graphene.

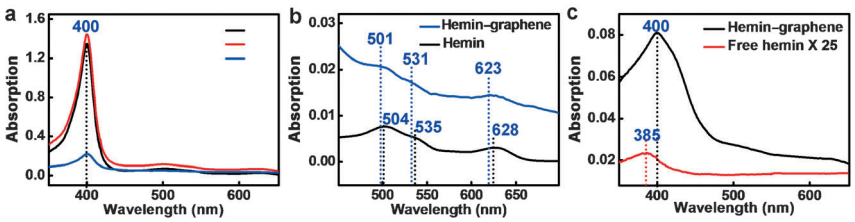

Figure 2. Characterization of hemin–graphene conjugates. a) UV/Vis spectroscopy of free hemin (black line), a hemin/graphene mixture (red line), and separated hemin–graphene re-dispersed in methanol solution (blue line). All samples show a Soret band at 400 nm. b) UV/Vis spectroscopy of free hemin, and hemin–graphene conjugates in methanol solution shows that the Q bands and charge-transfer (CT) band are slight blue-shifted upon formation of hemin–graphene conjugates. c) UV/Vis spectroscopy of free hemin and hemin–graphene conjugates in pH 7.4 Tris buffer, highlighting that the hemin retains monomeric form in the hemin–graphene conjugates, whereas free hemin in water forms catalytic inactive dimers.

To evaluate their catalytic activity, hemin–graphene conjugates were used as catalysts for the pyrogallol oxidation reaction (Figure 4a).[5a] The pyrogallol oxidation reaction, in which pyrogallol is oxidized into purpurogallin by hydrogen peroxide, is a commonly used standard assay to characterize the catalytic performance of various porphyrin derivatives.[5a] The catalytic reactions were carried out with a constant

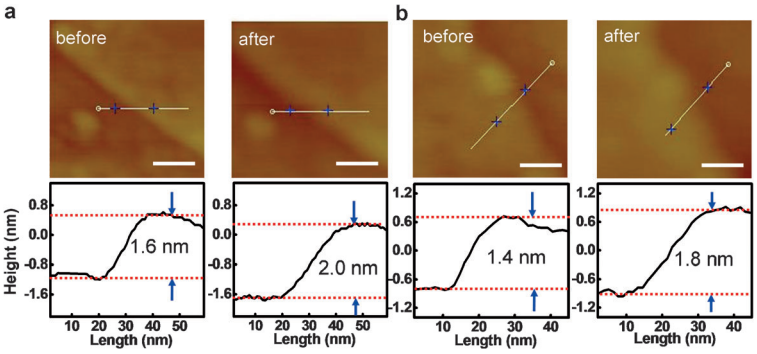

Figure 3. AFM morphology for hemin–graphene conjugates. The scale bars are 50 nm. The grahene flakes show a ca. 0.4 nm increase in step height after immersing into a hemin solution, which can be attributed to the absorption of a hemin monolayer.

© 2012 Wiley-VCH Verlag GmbH & Co. KGaA, Weinheim

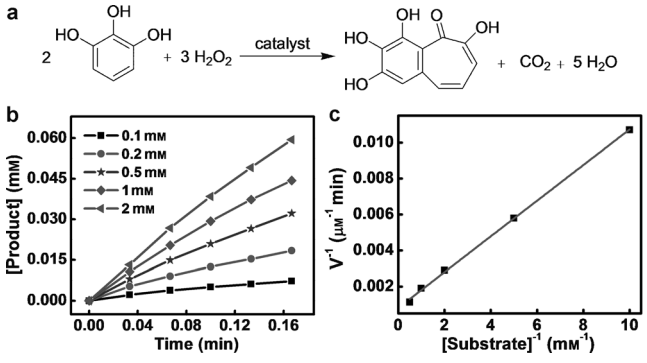

Figure 4. Oxidation reaction of pyrogallol catalyzed by hemin–graphene conjugates. a) Oxidation reaction of pyrogallol, in which pyrogallol is oxidized to purpurogallin by hydrogen peroxide. b) The initial pyrogallol oxidation profile catalyzed by hemin–graphene conjugates (5 μM hemin equivalent). The concentrations of pyrogallol range from 0.1 to 2 mM. c) Lineweaver–Burk plot of the pyrogallol oxidation catalyzed by the hemin–graphene conjugates.

hemin–graphene catalyst concentration (5 μM hemin equivalent), variable pyrogallol concentrations of 0.1–2 mM and a hydrogen peroxide concentration of 40 mM. The reaction progress was monitored at 420 nm by kinetic mode UV/Vis spectroscopy. The reaction process follows the conventional enzymatic dynamic regulation of the Michiaelis–Menten equation (Figure 4b). Based on the different oxidation rates with variable substrate concentrations, a Lineweaver–Burk plot can be obtained with a nearly perfect linear relationship (Figure 4c), from which the important kinetic parameters such as k_{cat} and K_M can be derived (Table 1). The k_{cat} value gives a direct measure of the catalytic production of the product, that is, it measures the maximum number of substrate molecules turned over per catalyst molecule per unit time under optimal conditions. It can also be viewed as the optimum turnover rate. K_M is the Michaelis constant and is often associated with the affinity of the catalyst molecules for the substrate. K_M is also a measure of the substrate concentration required for effective catalysis to occur. In this way, k_{cat}/K_M gives a measure of the catalytic efficiency. Either a large value of k_{cat} (rapid turnover) or a small value of K_M (high affinity for the substrate) will make k_{cat}/K_M large enough to obtain improved catalyst efficiency.

Table 1: Kinetic parameters for the pyrogallol oxidation reaction catalyzed using different catalysts.

Entry	Catalyst	k_{cat} [min^{-1}]	K_M [mM]	k_{cat}/K_M [$M^{-1} min^{-1}$]
1	hemin–graphene	246	1.22	2.0×10^5
2	hemin–hydrogel[5a]	19		
3	hemin[5b]	2.4		
4	FeTMPyP–graphene	545	0.96	5.7×10^5
5	FeTMPyP[6]	83		
6	FeTMPyP–antibody[6]	680	8.6	7.9×10^4
7	HRP[6]	1750	0.81	2.2×10^6

The derived k_{cat} of the hemin–graphene catalyst shows a surprisingly high value of 246 min^{-1}, which is more than one order of magnitude higher than a recently reported k_{cat} of a hemin–hydrogel catalyst (19 min^{-1}) and about two orders of magnitude higher than that of free hemin (2.4 min^{-1}) (Table 1). This k_{cat} value is nearly comparable to that of the natural enzyme horseradish peroxidase (HRP, around 1750 min^{-1}). The derived K_M value (around 1.2 mM) is also comparable to that of the natural enzyme HRP (0.81 mM), indicating a good affinity of the substrate to the hemin–graphene conjugates. Together, these studies clearly demonstrate that the hemin–graphene catalyst shows an excellent catalytic efficiency ($k_{cat}/K_M \approx 2\times10^5$), approaching that of the natural enzyme HRP ($k_{cat}/K_M \approx 2\times10^6$).

Other porphyrin derivatives such as FeTMPyP have also been explored as alternatives to hemin molecules with improved catalytic performance.[6] To demonstrate the general applicability of a graphene support to enhance the catalytic performance of porphyrin derivatives, we have synthesized FeTMPyP and immobilized them onto graphene using a similar method. Catalytic studies of the pyrogallol oxidation reaction with a FeTMPyP–graphene catalyst show similar behavior to that of the hemin–graphene catalyst (Figure 5a). The Lineweaver–Burk plot (Figure 5b) gives a k_{cat} value of 545 min^{-1}, which is comparable to that of the complex antibody-supported species (680 min^{-1}). More notably, the K_M of FeTMPyP–graphene (0.96 mM) is much lower than that of the antibody-supported species (8.6 mM), and it is similar to that of the natural enzyme HRP (0.81 mM), thus showing an excellent binding affinity. The catalytic efficiency (k_{cat}/K_M) of FeTMPyP–graphene ($5.7\times10^5\,M^{-1}min^{-1}$) is also about one order of magnitude better than that of the antibody-supported species ($7.9\times10^4\,M^{-1}min^{-1}$) and is nearly comparable to that of the natural enzyme HRP ($k_{cat}/K_M \approx 2\times10^6$). Overall, the FeTMPyP–graphene catalyst shows a further improvement in the catalytic performance, closely approaching the natural enzyme systems.

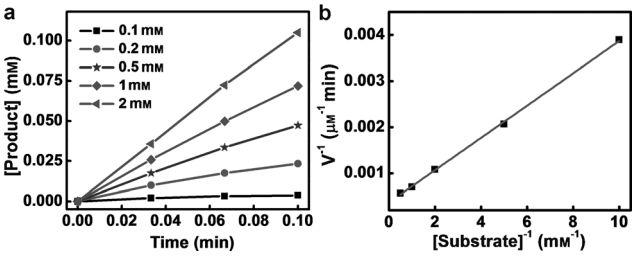

Figure 5. Pyrogallol oxidation catalyzed by FeTMPyP–graphene conjugates. a) Initial pyrogallol oxidation profile catalyzed by FeTMPyP–graphene (5 μM FeTMPyP equivalent). The concentrations of pyrogallol range from 0.1 to 2 mM. b) A Lineweaver–Burk plot of pyrogallol oxidation catalyzed by FeTMPyP–graphene.

Hemin–graphene conjugates have been prepared and explored as catalysts recently.[11c] However, the hemin–graphene conjugates obtained in this previous study have a dimeric form, with a catalytic activity comparable to that of free hemin (e.g. V_{max} of $4.55\times10^{-8}\,M\,s^{-1}$ for dimeric hemin–graphene vs. $4.69\times10^{-8}\,M\,s^{-1}$ for free hemin in the oxidation reaction of tetramethylbenzidine, TMB).[11c] We have also conducted the oxidation reaction of pyrogallol using free hemin or dimeric hemin–graphene conjugates, prepared by the reported approach, as catalysts. Neither of the two catalysts showed a measurable catalytic activity in the

 © 2012 Wiley-VCH Verlag GmbH & Co. KGaA, Weinheim

pyrogallol assay. Overall, the catalytic activity of the dimeric hemin–graphene is comparable to that of free hemin, and does not show apparent performance enhancement, whereas that of our monomeric hemin–graphene conjugates is at least 100 times more active than free hemin or dimeric hemin on graphene reported recently. These studies clearly highlight the importance to retain the monomeric hemin–graphene structure in the hemin–graphene conjugates.

Together, our studies demonstrate that graphene-supported porphyrin derivatives show excellent catalytic characteristics that are more than two orders of magnitude better than free hemin, and more than one order of magnitude better than any other supported system, which opens up new perspectives for other important oxidation reactions such as epoxidation and sulfoxidation. Our related studies have also shown that the hemin–graphene conjugate functions as an effective catalyst to facilitate the oxidation reaction of L-arginine (for nitric oxide generation) and the oxidation reaction of toluene. The fundamental reason for such a substantial enhancement of catalytic activity is a particularly interesting topic to be investigated in the future both experimentally and theoretically. In general, several combined features of the graphene support may contribute to the performance enhancement. First, graphene-supported hemin or FeTMPyP could prevent molecules from self-dimerization to form catalytically inactive species. Second, graphene as a support can block one side of the porphyrin molecule which could prevent hydrogen peroxide attack from both sides, and thus lowering the possibility of oxidative destruction of the catalyst molecules themselves.[16] Third, compared to a hydrogel support and other three-dimensional (3D) porous supports, graphene provides a two-dimensional (2D) support with a large open and accessible surface area; therefore, the diffusion of the substrate and product away from the catalytic centers is much easier, which could be beneficial to the reaction turnover rate and the binding interactions. Previous studies also demonstrated that a metalloporphyrin immobilized on a silica surface showed a higher catalytic activity than those trapped in a 3D silica matrix.[17] Fourth, graphene can function as a π donor to the iron centers of hemin through cation–π interactions. The cation–π interaction between the iron centers and graphene mimics the role of cysteine or histidine in enzymes, which have been proven as axial ligands to the hemin center from a Glu mutation study.[18] Enzymatic studies[19] also showed that axial ligands can serve multiple functions to enhance the catalytic characteristics, such as enhancement of the rate of O–O cleavage, promotion of heterolytic splitting rather than homolytic O–O splitting,[20] and stabilization of the ferryl (FeO^{4+}) moiety because of resonance and enhanced electrophilicity, which is crucial for the catalytic activity.[21]

Received: November 29, 2011
Revised: February 2, 2012
Published online: February 24, 2012

Keywords: biomimetic catalysis · enzymes · graphene · redox chemistry

[1] Z. Genfa, P. K. Dasgupta, *Anal. Chem.* **1992**, *64*, 517–522.
[2] T. C. Bruice, *Acc. Chem. Res.* **1991**, *24*, 243–249.
[3] a) D. Mansuy, *Coord. Chem. Rev.* **1993**, *125*, 129–141; b) M. Shema-Mizrachi, G. M. Pavan, E. Levin, A. Danani, N. G. Lemcoff, *J. Am. Chem. Soc.* **2011**, *133*, 14359–14367.
[4] F. Bedioui, *Coord. Chem. Rev.* **1995**, *144*, 39–68.
[5] a) Q. G. Wang, Z. M. Yang, X. Q. Zhang, X. D. Xiao, C. K. Chang, B. Xu, *Angew. Chem.* **2007**, *119*, 4363–4367; *Angew. Chem. Int. Ed.* **2007**, *46*, 4285–4289; b) Q. Wang, Z. Yang, M. Ma, C. K. Chang, B. Xu, *Chem. Eur. J.* **2008**, *14*, 5073–5078.
[6] H. Yamaguchi, K. Tsubouchi, K. Kawaguchi, E. Horita, A. Harada, *Chem. Eur. J.* **2004**, *10*, 6179–6186.
[7] a) A. K. Geim, K. S. Novoselov, *Nat. Mater.* **2007**, *6*, 183–191; b) F. Schwierz, *Nat. Nanotechnol.* **2010**, *5*, 487–496; c) J. Bai, R. Cheng, F. Xiu, L. Liao, M. Wang, A. Shailos, K. L. Wang, Y. Huang, X. Duan, *Nat. Nanotechnol.* **2010**, *5*, 655–659; d) L. Liao, Y.-C. Lin, M. Bao, R. Cheng, J. Bai, Y. Liu, Y. Qu, K. L. Wang, Y. Huang, X. Duan, *Nature* **2010**, *467*, 305–308.
[8] a) S. Park, R. S. Ruoff, *Nat. Nanotechnol.* **2009**, *4*, 217–224; b) M. J. Allen, V. C. Tung, R. B. Kaner, *Chem. Rev.* **2010**, *110*, 132–145; c) L. Jiao, L. Zhang, X. Wang, G. Diankov, H. Dai, *Nature* **2009**, *458*, 877–880.
[9] a) S. Stankovich, D. A. Dikin, R. D. Piner, K. A. Kohlhaas, A. Kleinhammes, Y. Jia, Y. Wu, S. T. Nguyen, R. S. Ruoff, *Carbon* **2007**, *45*, 1558–1565; b) D. Li, M. B. Mueller, S. Gilje, R. B. Kaner, G. G. Wallace, *Nat. Nanotechnol.* **2008**, *3*, 101–105; c) B. Y. Dai, L. Fu, L. Liao, N. Liu, K. Yan, Y. S. Chen, Z. F. Liu, *Nano Res.* **2011**, *4*, 434–439; d) V. C. Tung, J.-H. Huang, I. Tevis, F. Kim, J. Kim, C.-W. Chu, S. I. Stupp, J. Huang, *J. Am. Chem. Soc.* **2011**, *133*, 4940–4947; e) Y. Liang, Y. Li, H. Wang, J. Zhou, J. Wang, T. Regier, H. Dai, *Nat. Mater.* **2011**, *10*, 780–786.
[10] a) Y. Xu, L. Zhao, H. Bai, W. Hong, C. Li, G. Shi, *J. Am. Chem. Soc.* **2009**, *131*, 13490–13497; b) J. Geng, H.-T. Jung, *J. Phys. Chem. C* **2010**, *114*, 8227–8234; c) A. Ghosh, K. V. Rao, S. J. George, C. N. R. Rao, *Chem. Eur. J.* **2010**, *16*, 2700–2704; d) Y. Guo, L. Deng, J. Li, S. Guo, E. Wang, S. Dong, *Acs Nano* **2011**, *5*, 1282–1290.
[11] a) J. Chen, L. Zhao, H. Bai, G. Shi, *J. Electroanal. Chem.* **2011**, *657*, 34–38; b) S. Zhang, S. Tang, J. Lei, H. Dong, H. Ju, *J. Electroanal. Chem.* **2011**, *656*, 285–288; c) C. X. Guo, Y. Lei, C. M. Li, *Electroanalysis* **2011**, *23*, 885–893.
[12] W. S. Hummers, R. E. Offeman, *J. Am. Chem. Soc.* **1958**, *80*, 1339–1339.
[13] E. S. Ryabova, A. Dikiy, A. E. Hesslein, M. J. Bjerrum, S. Ciurli, E. Nordlander, *J. Biol. Inorg. Chem.* **2004**, *9*, 385–395.
[14] E. Droghetti, S. Sumithran, M. Sono, M. Antalik, M. Fedurco, J. H. Dawson, G. Smulevich, *Arch. Biochem. Biophys.* **2009**, *489*, 68–75.
[15] J. Silver, B. Lukas, *Inorg. Chim. Acta Bioinorg. Chem.* **1983**, *78*, 219–224.
[16] V. Ullrich, *Arch. Biochem. Biophys.* **2003**, *409*, 45–51.
[17] M. S. M. Moreira, P. R. Martins, R. B. Curi, O. R. Nascimento, Y. Iamamoto, *J. Mol. Catal. A* **2005**, *233*, 73–81.
[18] G. Smulevich, F. Neri, O. Willemsen, K. Choudhury, M. P. Marzocchi, T. L. Poulos, *Biochemistry* **1995**, *34*, 13485–13490.
[19] a) M. C. Feiters, A. E. Rowan, R. J. M. Nolte, *Chem. Soc. Rev.* **2000**, *29*, 375–384; b) K. Szaciłowski, A. Chmura, Z. Stasicka, *Coord. Chem. Rev.* **2005**, *249*, 2408–2436.
[20] D. Harris, G. Loew, L. Waskell, *J. Am. Chem. Soc.* **1998**, *120*, 4308–4318.
[21] a) F. A. Walker, *J. Inorg. Biochem.* **2005**, *99*, 216–236; b) A. Weichsel, E. M. Maes, J. F. Andersen, J. G. Valenzuela, T. K. Shokhireva, F. A. Walker, W. R. Montfort, *Proc. Natl. Acad. Sci. USA* **2005**, *102*, 594–599.

 © 2012 Wiley-VCH Verlag GmbH & Co. KGaA, Weinheim